# Safe Navigation of a Mobile Robot Considering Visibility of Environment

Woojin Chung, *Member, IEEE*, Seokgyu Kim, Minki Choi, Jaesik Choi, Hoyeon Kim, Chang-bae Moon, and Jae-Bok Song, *Member, IEEE*

***Abstract*—We present one approach to achieve safe navigation in an indoor dynamic environment. So far, there have been various useful collision avoidance algorithms and path planning schemes. However, those algorithms possess fundamental limitations in that the robot can avoid only "visible" ones among surrounded obstacles. In a real environment, it is not possible to detect all the dynamic obstacles around the robot. There are many occluded regions due to the limited field of view. In order to avoid collisions, it is desirable to exploit visibility information. This paper proposes a safe navigation scheme to reduce collision risk considering occluded dynamic obstacles. The robot's motion is controlled by the hybrid control scheme. The possibility of collision is dually reflected to path planning and speed control. The proposed scheme clearly indicates the structural procedure on how to model and to exploit the risk of navigation. The proposed scheme is experimentally tested in a real office building. The experimental results show that the robot moves along the safe path to obtain sufficient field of view. In addition, safe speed constraints are applied in motion control. It is experimentally verified that a robot safely navigates in dynamic indoor environment by adopting the proposed scheme.**

***Index Terms*—Mobile robot navigation, obstacle avoidance, path planning, speed control.**

## I. Introduction

FROM THE viewpoint of autonomous navigation, safety in a human coexisting environment is an essential problem. On the other hand, high-speed navigation is preferable in order to increase service efficiency. In order to achieve high-speed navigation, some limitations should be taken into account as follows:

1) dynamic and mechanical limitations;
2) control and computational limitations;
3) unexpected dynamic change of environment.

The first problem implies wheel slippage or rollover when a robot makes a sharp cornering or an emergency stop. In practical applications, the first problem is rarely considered because other problems cause more strict limitations on the maximum speed of the mobile robot.

The second problem can be interpreted as a real-time obstacle avoidance problem. Navigation speed is limited by sensing accuracy, processing speed, computational cost, and motion control response. Kanayama *et al.* proposed a trajectory tracking algorithm of two wheel differential mobile robots in [1] which guarantees the exponential convergence. Macek *et al.* proposed a control method for stable and smooth path following algorithm in [2] based on the Virtual Vehicle Approach [3]. Fox *et al.* proposed the dynamic window approach (DWA) in [4] based on the curvature velocity method [5]. The DWA is particularly useful when the robot navigates in dynamic obstacle environment. Seder and Petrovic [6] proposed the modified DWA algorithm based on the integration of focused $D^*$ search algorithm in [7] considering moving obstacles. Their work showed improved obstacle avoidance performance by predicting the obstacle motions. Minguez *et al.* proposed the nearness diagram (ND) approach in [8]. ND shows superior performance particularly in a highly cluttered environment. Quinlan [9] proposed path deformation technique that works in real time when obstacles block the original path. Montesano *et al.* addressed the problem of modeling obstacles, and integration of obstacle information in a local motion planning in [10]. A mobile robot can avoid "visible" obstacles by adopting existing technologies.

Our major scope in this paper is to solve the third problem addressed above. Suppose that a person drives along a narrow road without any traffic signals. He may reduce speed when approaching a junction. It is natural to assume that there might be dynamic obstacles in occluded regions. Sometimes a driver chooses a detour path to obtain sufficient field of view. The purpose of this paper is to derive the risk of potential collision with occluded dynamic obstacles, and to establish a general control scheme to cope with the risk.

There have been some works to deal with unexpected collision and visibility problems. Sadou *et al.* [11] focused on the occluded obstacles. The scope of unexpected obstacles is

Manuscript received June 14, 2008; revised June 1, 2009. First published June 23, 2009; current version published September 16, 2009. This work was supported in part by Dasa Robot Corporation as a part of project "Development of Patrol and Safety Service Robot Systems," by the KOSEF Grant funded by the MEST (R01-2008-000-11995-0), by the MKE under the Human Resources Development Program for Convergence Robot Specialists, by the MKE under the ITRC support program [IITA-2008-(C1090-0803-0006)], and by the Intelligent Robotics Development Program, one of the 21st Century Frontier R&D Programs funded by MKE.

W. Chung, M. Choi, H. Kim, C. Moon, and J.-B. Song are with the Department of Mechanical Engineering, Korea University, Seoul 136-713, Korea (e-mail: smartrobot@korea.ac.kr; taewonii@hanafos.com; yongbe@korea.ac.kr; lunar@teramail.com; jbsong@korea.ac.kr).

S. Kim was with the Department of Mechanical Engineering, Korea University, Seoul 136-713, Korea. He is now with the Corporate Research and Development Division, Hyundai–Kia Motors, Gyeonggi-do 445-706, Korea (e-mail: seokgyu.kim@hyundai-motor.com).

J. Choi was with the Department of Mechanical Engineering, Korea University, Seoul 136-713, Korea. He is now with the Department of Computer Science, University of Illinois at Urbana–Champaign, Urbana, IL 61801 USA (e-mail: jaesik.choi@gmail.com).

Color versions of one or more of the figures in this paper are available online at http://ieeexplore.ieee.org.

Digital Object Identifier 10.1109/TIE.2009.2025293

limited to the occluded obstacles on the path, and the path is always fixed. Another approach is to utilize navigation experiences to predict the human walking pattern in [12]. It was shown that the robot can provide appropriate mobile services by monitoring and utilizing patterns of people. The work in [12] shows an example to deal with environmental changes. Krishna *et al.* [13] computed the safe velocity profile along the path and modified the path near the occluded region. The work also shows a speed control strategy for safety. However, it is required to develop a general approach to combine the path planning and the speed control to cope with occluded dynamic obstacles. Another example of speed control can be found in [14]. Well-defined speed constraints are established considering vehicle features in [14]. However, there is no scheme for path modification. The major advantage of this paper is to suggest a generalized procedure to deal with both path planning and speed control.

In this paper, we establish a safe navigation scheme from two aspects. The first aspect is path planning. Most of the existing path planners only focus on detectable obstacles. In addition, the optimality is defined in terms of moving distance in conventional planners. However, the shortest path is not necessarily safe in many cases. It will be shown that the path planner should reflect the risk of possible collision with occluded obstacles. The collision risk is quantitatively modeled through the intrinsic cost of the gradient method, which was introduced in [15].

The second aspect is deriving speed constraints. Once a robot's path is given, allowable maximum speed can be explicitly derived. The speed constraint is applied through the DWA in [4]. The specific criterion on deciding maximum velocity was an open problem in [4]. This paper derives an explicit condition on the maximum speed in order to avoid collision. A part of this paper was introduced in [16]. Related navigation issues including localization and control architecture design can be seen in [17]–[19]. In those works, development of the multifunctional mobile service robot was presented. The integrated localization strategy was developed based on laser range finder readings. The architecture is a hybrid reactive-deliberate scheme including the Petri Net-based behavior selection control scheme. Some recent robotic applications can be found in [22]–[24].

In this paper, we propose a structural navigation scheme importing the potential collision risks by considering the visibility information without loss of generality. Previous obstacle avoidance techniques deal with detected moving obstacles. The idea of this paper is that it is worth considering the field of view limitations of sensors and the collision risk by occluded moving obstacles. In this paper, we quantitatively derive the collision risk and establish path optimization and speed control strategies. The proposed scheme will be experimentally verified.

This paper is organized as follows. Section II describes how to compute occluded regions and the risk of unexpected collision. Then, we propose path planning and motion control schemes to achieve safe navigation. Simulations and experimental verifications are made in Section III. Some concluding remarks are given in Section IV.

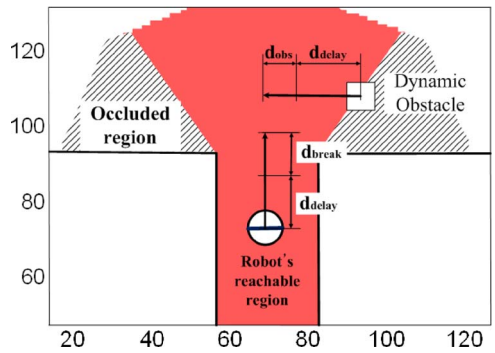


Fig. 1. Occluded reachable regions and a dynamic obstacle.

## II. Navigation Risk Modeling Considering Visibility

### A. Collision Risk Due to Occlusion

Once we have an environmental map, we can find the region where the field of view is geometrically obstructed. Considering the dynamic capacity of a robot and the speed of a dynamic obstacle, the collision distance can be computed as the following:

$$d_{\text{delay}} = t_{\text{delay}} \times (v_{\text{r}} + v_{\text{obs}}) \tag{1}$$

$$d_{\text{break}} = v_{\text{r}}^2/(2 \times a_{\text{robot}}) \tag{2}$$

$$d_{\text{obs}} = v_{\text{obs}} \times v_{\text{r}}/a_{\text{robot}} \tag{3}$$

$$d_{\text{collision}} = d_{\text{delay}} + d_{\text{break}} + d_{\text{obs}}. \tag{4}$$

The collision distance $d_{\text{collision}}$ implies the minimum clearance which should be guaranteed to avoid collision with a dynamic obstacle. The robot should be able to make a complete emergency stop in the range of $d_{\text{collision}}$. $d_{\text{delay}}$ is caused by the time delay of sensors and controllers after detecting an obstacle around the robot. $d_{\text{break}}$ is a breaking distance of a robot, and it is determined by the dynamic control performance of a robot. $d_{\text{obs}}$ is the moving distance of the obstacle during the deceleration time of a robot before making a complete stop. Fig. 1 shows the conceptual illustration of $d_{\text{collision}}$. $v_{\text{r}}$, $v_{\text{obs}}$, and $a_{\text{robot}}$ are the speed of a robot, the speed of an obstacle, and the acceleration of a robot, respectively.

Fig. 1 shows the risk of potential collision with dynamic obstacles from occluded regions when a robot approaches a junction. Fig. 1 also shows a reachable region of a robot when $v_{\text{r}} = 1$ m/s and $v_{\text{obs}} = 4$ m/s. Since the exact computation of nonholonomic robot's reachable region is computationally expensive, we have adopted the wavefront propagation algorithm in [20] for approximate computation of reachable regions.

The occluded area is defined as the difference between the reachable area and the visible area. The reachable area is the robot's neighborhood considering $d_{\text{collision}}$. The visible area is computed by the ray tracing method. The occluded reachable region of a robot can be considered as a risky area. The risky position is calculated from the collision distance $d_{\text{collision}}$ using (4). In most cases, $a_{\text{robot}}$ and $t_{\text{delay}}$ can be assumed to be constants. Therefore, the risky area is dependent on $v_{\text{r}}$ and $v_{\text{obs}}$.

The existence of occluded regions over the entire workspace can be easily obtained. When the occluded area exists, the robot

(a)

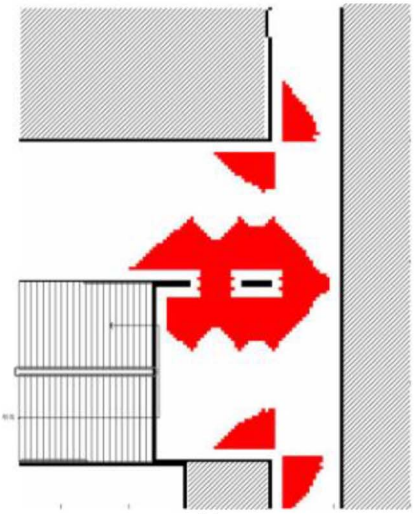

(b)

Fig. 2. Computation of regional risk due to potential collision. (a) Real environment. (b) Computed risky area due to occlusion.

position is registered as a risky position. Therefore, the set of risky positions is registered to a map. This step corresponds to a preprocessing step to model the risk of collision.

Fig. 2(a) shows real environment in a conventional office building. Fig. 2(b) shows the computed risky regions. It is clear that the risky regions are located around the corner or a pillar. The computational result matches well with our daily experience on the risky area, where unexpected collisions might take place.

### B. Speed Constraints

Real environments are mostly polygonal, and there are some particular points which limit visibility. More specifically, convex edges are extreme points which limit field of view, as shown in Fig. 1(a). With the environmental map, convex edges can be easily extracted.

Fig. 3 shows the convex edges. One of the most dangerous cases is that the dynamic obstacle directly moves to the robot from the occluded area. The convex edge is the closest point of the occluded region from a robot. The robot is collision-free when the robot stands far away from the convex edge than the collision distance. A similar motion model of obstacles can be found in [13]. In [13], under the assumption that collision takes place at the intersection of the circle and the path, a safe speed

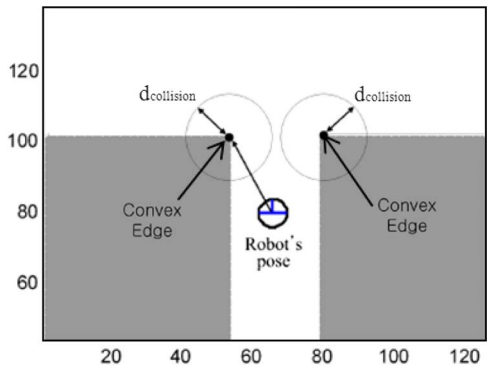


Fig. 3. Convex edges and collision distance.

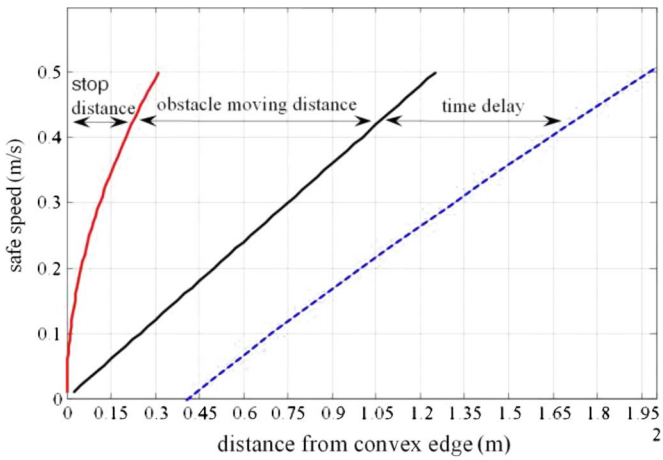


Fig. 4. $d_{\mathrm{collision}}$ versus maximum safe speed of a robot.

is derived. In this paper, considering more conservative case, the distance from a robot to a convex edge is taken into account to define a safe speed.

Fig. 4 shows the relationship between the clearance to the convex edge and the robot's maximum speed. The convex edge is considered to be the starting position of a dynamic obstacle. The sampling rate of a control loop is about 0.2 s. We assumed that the obstacle speed is 2 m/s, $d_{\mathrm{delay}}$ is about 0.4 m when the robot speed is zero. This result is shown in Fig. 4. When we want to drive a robot faster than 0.3 m/s, we can conclude that the clearance should be always greater than 1.35 m from Fig. 4. Therefore, $d_{\mathrm{collision}}$ can be understood as the distance margin before collision.

The computational result of safe speed from all convex edges is shown in Fig. 5. The environment is identical with the environment in Fig. 2. The result shows that a robot should move slowly near the convex edge. If the robot moves far away from convex edges of the environment, the robot can speed up to its mechanical limit.

### C. Risky Regions With Speed Constraints

After deriving the risky regions and speed constraints, that information should be merged by taking the intersection. The maximum speed condition at the risky area shows quantitative risk of collision.

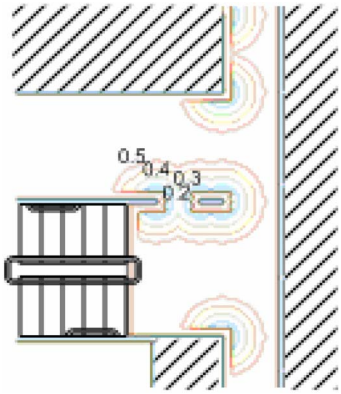


Fig. 5. Computed maximum speed to guarantee safety (in meters per second).

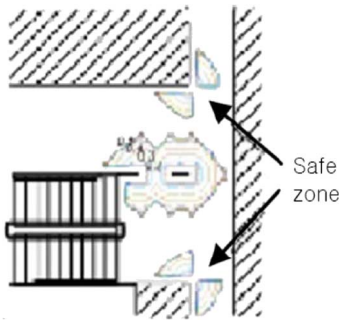


Fig. 6. Risky area with safe speed constraint.

The computational result of association is shown in Fig. 6. In general, the close neighborhood of the convex edge is dangerous. However, there are some safe zones around the convex edge, as shown in Fig. 6, because the field of view is not limited.

### D. Path Planning and Motion Control

There are some possible alternatives to reflect environment risks. First, collision risk can be considered in path planning. Second, the distance margin can be used in motion control as a maximum speed limitation. Our navigation strategy is a hybrid approach to combine path planning and reactive control, as in [21]. The path planner is designed based on the gradient method in [15]. The reactive motion controller is the DWA in [4].

The gradient method path planning [15] generates a minimum distance path without local minima. Path cost $F(P)$ is computed as the sum of intrinsic cost and adjacency cost as a following equation:

$$F(P) = \sum_i I(P_i) + \sum_i A(P_i, P_{i+1}). \tag{5}$$

$P_i$ indicates grids in unoccupied free space. Intrinsic cost at $P_i$, $I(P_i)$ can be assigned high near an obstacle or slippery region. Adjacency cost $A(P_i, P_{i+1})$ is proportional to moving distance.

Our approach is to use the distance margin and the visibility information in the gradient method. The gradient method provides a general framework to model risks through the intrinsic cost. Therefore, the distance margin is mapped into the intrinsic cost. In this paper, the intrinsic cost is proportional to the reciprocal of the maximum speed. As a result, the minimum time path can be obtained. There are some possible indices for path optimization. Performance indices can be minimum energy, minimum distance, or minimum time. We adopt the minimum time criterion in order to increase the service efficiency of a robot under the condition that safety is always guaranteed.

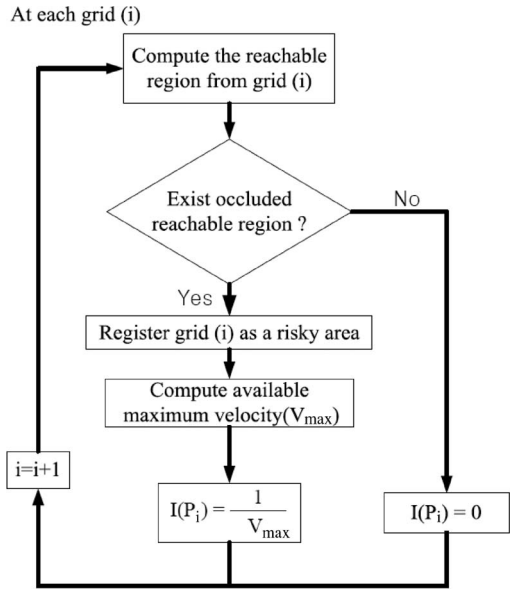


Fig. 7. Algorithmic flow to compute the risk of grids.

The procedure to model regional risks of navigation is summarized in Fig. 7. Since the environment is described by a grid map, collision risk is iteratively computed for each grid. For grid $i$, the field of view limitation is computed first. If there is any occluded region, then grid $i$ is registered as a risky area. The next step is to derive maximum speed constraint by using (1)–(4). When the speed constraints are derived, the intrinsic cost of the gradient path planner is given by the reciprocal of the maximum speed. Finally, the optimal path can be obtained by applying the gradient path planner.

Our collision-free navigation scheme is designed based on global DWA in [21]. In DWA, the performance measure function is composed of three criteria. One of the criteria is the speed object, which encourages fast movement of the robot. The distance margin can be mapped into the speed object through the maximum speed.

## III. Simulation and Experiment Results

### A. Collision Risk Index and Experimental Conditions

It is necessary to define a performance measure to evaluate the safety during navigation. We define collision risk $I_{\text{collision}}$ as

$$I_{\text{collision}} = \frac{A_{\text{collision}}}{A_{\text{collision}} + A_{\text{safe}}}. \tag{6}$$

All areas are defined in the dynamic window. $A_{\text{collision}}$ and $A_{\text{safe}}$ indicate the area of collision and the area of admissible velocity, respectively. $I_{\text{collision}}$ varies from zero to one when the admissible collision-free velocity area becomes small. If $I_{\text{collision}}$ is close to one, most of the velocities in the dynamic

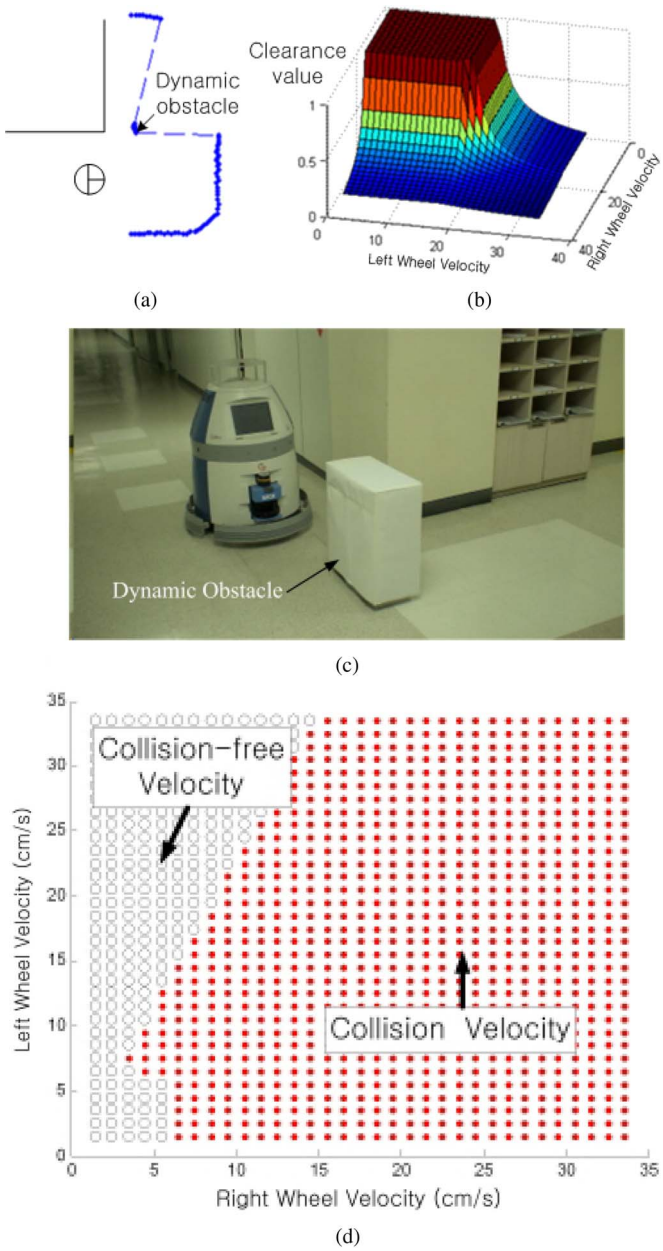


Fig. 8. Experiment to compute collision risk index $I_{\text{collision}}$. (a) Range sensor image. (b) Clearance object. (c) Robot's situation. (d) Collision velocity in the dynamic window.

window result in collision. Therefore, the navigation control scheme should be modified when $I_{\text{collision}}$ becomes close to one. For example, the cruising speed of a robot should be reduced. $I_{\text{collision}}$ is used to monitor the risk of collision in dynamic obstacle environment. It is desirable that $I_{\text{collision}}$ is close to zero for safe navigation.

Fig. 8 shows the collision risk of unexpected dynamic obstacle. Fig. 8(a) shows the sensor data when a dynamic obstacle exists in front of a robot. The clearance object in dynamic window is shown in Fig. 8(b). If the clearance object is smaller than the threshold 0.2, it is classified into the collision velocity region. Fig. 8(c) shows current locations of a robot and an obstacle. Collision velocity area is shown in Fig. 8(d). From Fig. 8(d), it is clear that the robot should turn right by accelerating the left wheel in order to avoid the obstacle. Collision velocity area is quite large and $I_{\text{collision}}$ is 0.78. Therefore, we can conclude that the robot is in a dangerous situation.

Experiments were carried out in an office building. Maximum speed of the robot was 0.5 m/s. Maximum acceleration of the robot was 0.8 $\text{m}/\text{s}^2$. Sampling time of the laser range finder was 0.2 s. Dynamic obstacles are mostly walking people. In general, the human's maximum walking speed is about 1 m/s in indoor environment. In order to allow some safety margin, the speed of dynamic obstacle was assumed to be 1.5–3 m/s in experiments. Experiments were carried out with three different boundary conditions: Hair-pin navigation, doorway navigation, and narrow area passing.

Three control schemes were applied for each experiment. One is the conventional gradient method combined with the conventional DWA. Therefore, the first controller does not consider the collision risk due to occlusion. The second controller is to add safe speed constraint along the conventional gradient path. Therefore, path modification for safety is not allowed. The third controller is the proposed path planner combined with safe speed constraints.

In experiments, a dynamic obstacle interrupts the robot's movement. A dynamic obstacle is another mobile robot. The obstacle starts from an occluded region and moves across the robot path.

We use a grid map for environmental representation. Since it is difficult to model the stairs automatically, the map for path planning was manually modified by setting the stairs as the obstacle region.

### *B. Experiment 1: Hair-Pin Navigation*

The first experiment is hair-pin navigation, and the experimental condition is shown in Fig. 9(a). In this experiment, the dynamic obstacle moves from A to B in 3 m/s. Fig. 9(b) shows the resultant trajectories. The conventional gradient path is represented by a solid line. Although the conventional path is the shortest one, the path passes through a close neighborhood of a wall. In case of the speed control, the robot moved along the generated gradient path under the proposed safe speed constraint. The robot stopped near the corner due to the speed limitation. Since the robot passed through highly risky area, the maximum speed reached zero. As a result, the robot stopped before reaching a goal. Therefore, the robot failed to accomplish the navigation task when speed constraints are applied to the conventional path.

Fig. 10 shows the speed and $I_{\text{collision}}$ during experiment 1. From Fig. 10(a), travel time using gradient method is 20.8 s and it is the fastest. However, $I_{\text{collision}}$ jumped when a robot encountered a dynamic obstacle around 8 s, as shown in Fig. 10(a). Therefore, it is clear that the conventional gradient path cannot guarantee collision safety in dynamic environment. The conventional gradient path should not be used in practical applications. Fig. 10(b) shows the resultant speed of a robot under the safe speed constraint. It is clear that $I_{\text{collision}}$ maintains zero owing to the slow speed. However, the robot failed to reach the goal due to stopping. Fig. 10(c) shows speed and $I_{\text{collision}}$ by the proposed method. As shown in Fig. 9(b), the path makes a detour to achieve sufficient field of view. $I_{\text{collision}}$

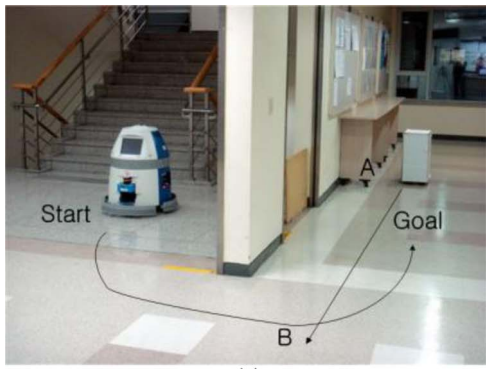


(a)

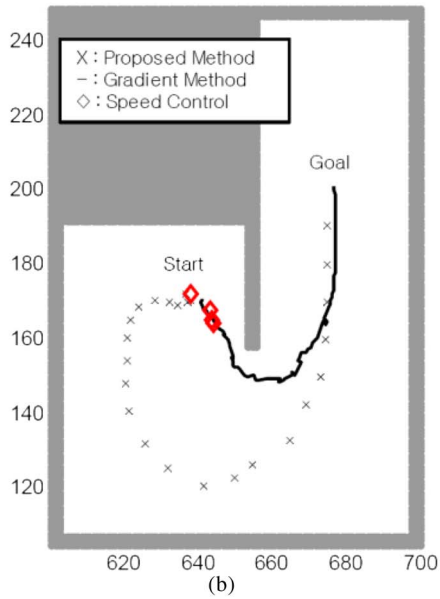


(b)

Fig. 9. Experiment 1: Hair-pin navigation. (a) Experimental environment and condition for experiment 1. (b) Resultant trajectories.

instantaneously increased to 0.42 around 31 s due to the dynamic obstacle. The robot could avoid an obstacle successfully, and the collision risk was low enough $(I_{\text{collision,max}} = 0.42)$ during the entire movement. In addition, the robot moved faster because the robot moved along the safe path. Although the travel time was over 40 s, it can be considered as the minimum time solution which satisfies safety. In Fig. 10(c), it is shown that the robot velocity fluctuates locally. The feasible maximum acceleration of a robot is 0.8 $\text{m/s}^2$ when we consider mechanical and dynamic properties of a robot. It is assumed that the autonomous robot independently moves without frequent human interaction. As a result, it is desirable to use maximum acceleration in order to increase the dynamic obstacle avoidance capability. Therefore, it is acceptable to show jerky velocity profiles locally.

### C. Experiment 2: Doorway Navigation

Experiment 2 is to pass through a doorway. In experiment 2, the dynamic obstacle moves from A to B in 1.5 m/s, as shown in Fig. 11(a). In Fig. 11(a), there is not much space for path deformation. Therefore, speed constraints play a dominant role to avoid collision. It is common to reduce robot's speed heuristically when a robot passes through the doorway. However,

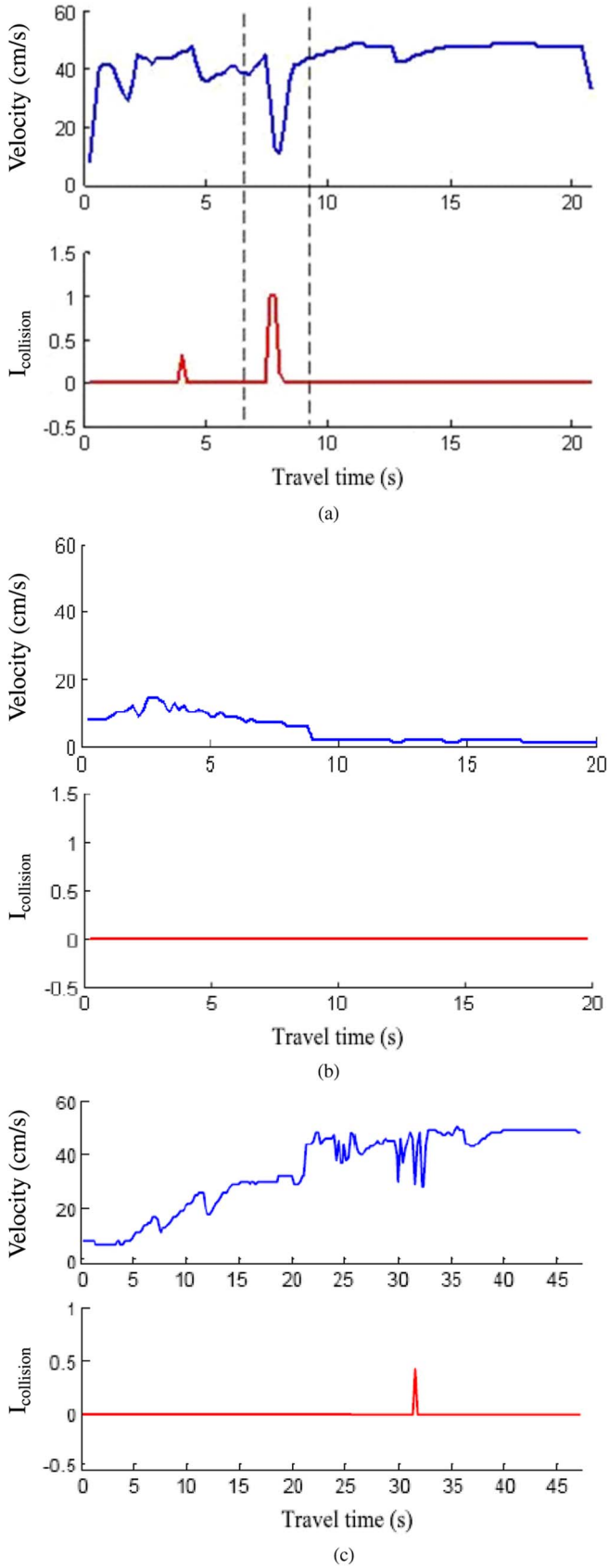


Fig. 10. Velocity and collision risk index during experiment 1. (a) Velocity and collision risk index along the conventional gradient path without considering collision risk. (b) Velocity and collision risk index along the conventional gradient path with the safe speed constraint. (c) Velocity and collision risk index along the proposed path with the safe speed constraint.

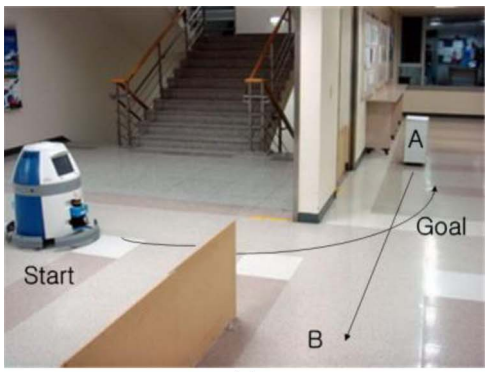


(a)

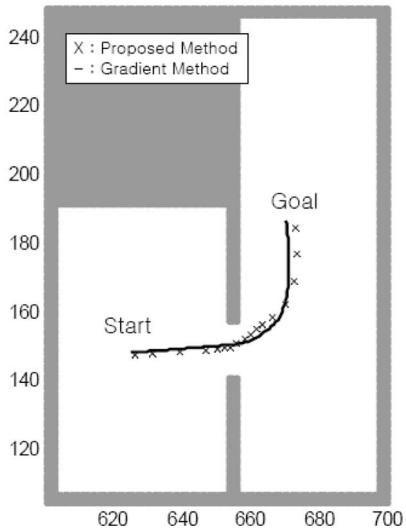


(b)

Fig. 11. Experiment 2: Doorway navigation. (a) Experimental environment and condition for experiment 2. (b) Resultant trajectories.

the robot speed is appropriately controlled with the proposed scheme without adding any heuristics, owing to the generality of the proposed scheme.

Fig. 11 shows the result that the proposed path is close to the conventional path. However, it is clear that a robot slowed down before entering the doorway due to the speed constraint.

Fig. 12(a) shows the velocity of a robot and $I_{\text{collision}}$ using the conventional gradient method. The $I_{\text{collision}}$ abruptly increases and the speed of a robot decreases when the robot encounters the dynamic obstacle around 6 s. The configurations of a robot and an obstacle around 6 s are shown in Fig. 6(b). The laser range data at the moment is shown in Fig. 6(c). Therefore, it is dangerous to adopt the conventional method in practical applications. Fig. 12(d) shows the velocity profile using the proposed method. When a robot moves in the outside of the risky area from 0 to 4 s, the speed is about 0.5 m/s. A robot passed through the doorway with reduced speed about 0.1 m/s due to the field of view limitation. The speed of the dynamic obstacle was assumed to be quite fast (1.5 m/s). $I_{\text{collision,max}}$ was 0.08 throughout the experiment. This fact implies that safe navigation can be achieved by speed control only. This result coincides with our daily experiences. If a car is parked at a narrow parking lot, a driver should be extremely careful and should reduce the speed in dynamic situations.

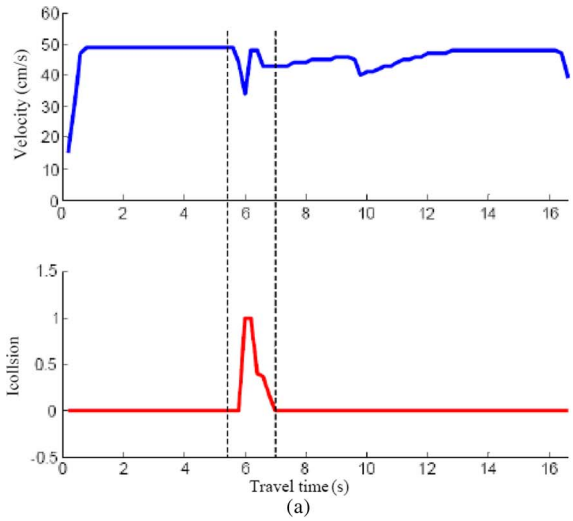


(a)

(b)

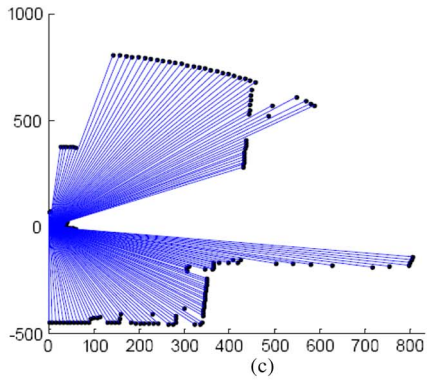

(c)

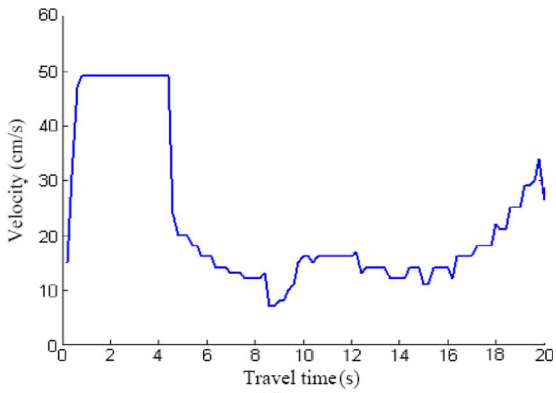


(d)

Fig. 12. Gradient velocity and collision risk index during experiment 2. (a) Velocity and collision risk index along the conventional gradient path without considering collision risk. Collision occurred around 6 s. (b) Robot is in collision with an obstacle by applying the conventional scheme. $I_{\text{collision}} = 1$ around 6 s. (c) Laser range data around 6 s. (d) Translational velocity of a robot by applying the proposed control scheme.

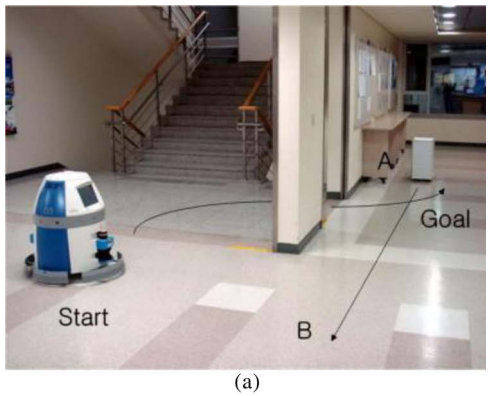


(a)

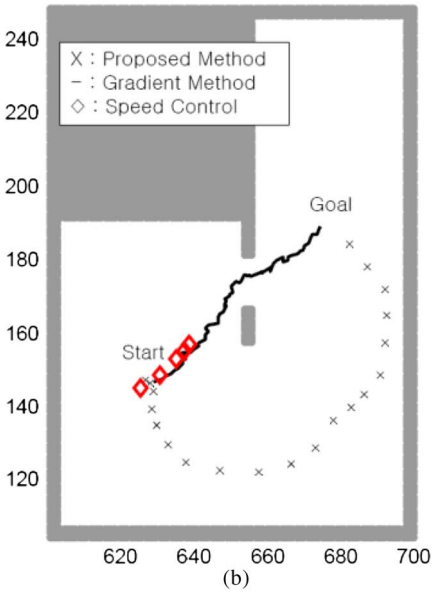


(b)

Fig. 13. Experiment 3: Passing through narrow area. (a) Experimental environment and condition for experiment 3. (b) Resultant trajectories.

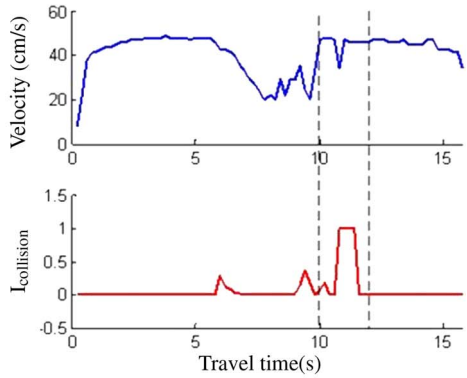


(a)

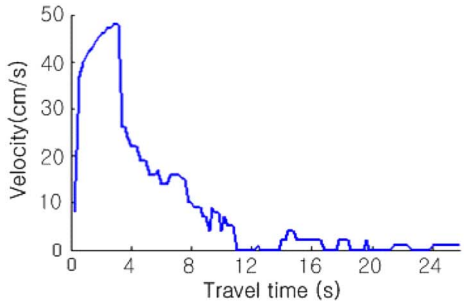


(b)

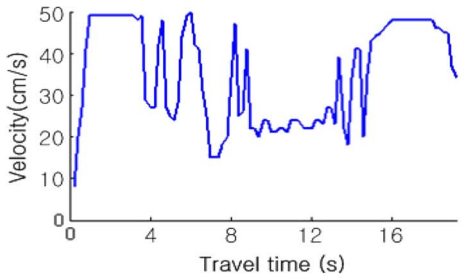


(c)

Fig. 14. Velocity and collision risk index during experiment 3. (a) Velocity and collision risk index along the conventional gradient path without considering collision risk. (b) Velocity along the gradient path with the safe speed constraint. (c) Velocity along the proposed path with the safe speed constraint.

### *D. Experiment 3: Passing Through Narrow Area*

Most of the conventional path planner provides the shortest path. However, the highest priority should be given to safety rather than the distance of travel. Fig. 13 shows the gradient path, which passes through the narrow area between a wall and a pillar. In experiment 3, the dynamic obstacle moves from A to B, as shown in Fig. 13(a). From Fig. 14(a), it is clear that the gradient path is dangerous because collision risk index reaches 1 around 11 s due to the dynamic obstacle. A robot stopped before entering the narrow area under the safe speed constraint, which is obvious from Fig. 14(b). Detoured paths are obtained when we apply the proposed method. If the robot tries to go through the narrow region, the robot speed decreases a lot, in order to prevent possible collision. Therefore, the shortest path requires longer travel time for a safe navigation. As a result, a detour path is safe and fast. It is clear that a robot moves fast along the detour path from Figs. 13(b) and 14(c). With the proposed controllers, $I_{\text{collision,max}}$ was 0.48 throughout the experiment.

Table I summarizes experimental results. As shown in Table I, the conventional gradient path shows the shortest total travel time. However, the conventional approach is not applicable because the peak collision risk is 1.0, which implies collision situation. Although it is safe to apply speed constraint along the conventional gradient path, the robot could not reach the goal because the available speed was almost zero. The robot could reach the goal safely when the proposed scheme was applied even though a dynamic obstacle disturbed robot's movement. Therefore, it can be concluded that it is safe to apply the proposed scheme.

TABLE I
EXPERIMENTAL RESULTS

| Experiments | | Conventional | Speed control only | Proposed |
|---|---|---|---|---|
| Hair-pin | $t_c$ | 20.8 | fail | 47 |
| | $I_{collision,\ max}$ | 1.0 | - | 0.42 |
| Doorway | $t_c$ | 16.4 | fail | 26.2 |
| | $I_{collision,\ max}$ | 1.0 | - | 0.08 |
| Narrow Area | $t_c$ | 15.6 | fail | 19.0 |
| | $I_{collision,\ max}$ | 1.0 | - | 0.48 |

* $t_c(s)$ total travel time, $I_{collision}$: Peak risk index

## IV. Conclusion

This paper presented a navigation scheme by considering the visibility information for safe and fast navigation. The environmental risks were quantitatively derived to deal with collision with occluded dynamic obstacles. The collision risk was quantitatively derived, and it was exploited both for path planning and the speed control in a structural way. The presented simulations and experimental results clearly showed that the proposed navigation scheme is an efficient and safe solution for indoor mobile robots.

## References


[1] Y. Kanayama, Y. Kimura, F. Miyazaki, and T. Noguchi, "A stable tracking control method for an autonomous mobile robot," in *Proc. IEEE Int. Conf. Robot. Autom.*, Cincinnati, OH, May 13–18, 1990, pp. 384–389.

[2] K. Macek, I. Petrovic, and R. Siegwart, "A control method for stable and smooth path following of mobile robots," in *Proc. Eur. Conf. Mobile Robots*, 2005, pp. 128–133.

[3] M. Egerstedt, X. Hu, and A. Stotsky, "Control of mobile platforms using a virtual vehicle approach," *IEEE Trans. Autom. Control*, vol. 46, no. 11, pp. 1777–1782, Nov. 2001.

[4] D. Fox, W. Burgard, and S. Thrun, "The dynamic window approach to collision avoidance," *IEEE Robot. Autom. Mag.*, vol. 4, no. 1, pp. 23–33, Mar. 1997.

[5] R. Simmons, "The curvature-velocity method for local obstacle avoidance," in *Proc. IEEE Int. Conf. Robot. Autom.*, Minneapolis, MN, Apr. 22–28, 1996, pp. 3375–3382.

[6] M. Seder and I. Petrovic, "Dynamic window based approach to mobile robot motion control in the presence of moving obstacles," in *Proc. IEEE Int. Conf. Robot. Autom.*, Roma, Italy, Apr. 10–14, 2007, pp. 1986–1991.

[7] A. Stentz, "The focusedD* algorithm for real-time preplanning," in *Proc. Int. Joint Conf. Artif. Intell.*, 1995, pp. 1652–1659.

[8] J. Minguez, L. Montano, T. Simeon, and R. Alami, "Global nearness diagram navigation (GND)," in *Proc. IEEE Int. Conf. Robot. Autom.*, Seoul, Korea, May 21–26, 2001, pp. 33–39.

[9] S. Quinlan, "Real-time modification of collision-free paths," Ph.D. dissertation, Stanford Univ., Stanford, CA, 1994.

[10] L. Montesano, J. Minguez, and L. Montano, "Modeling dynamic scenarios for local sensor-based motion planning," *Auton. Robots*, vol. 25, no. 3, pp. 231–251, Oct. 2008.

[11] M. Sadou, V. Polotski, and P. Cohen, "Occlusions in obstacle detection for safe navigation," in *Proc. IEEE Intell. Veh. Symp.*, 2004, pp. 716–721.

[12] M. Bennewitz, W. Burgard, G. Cielniak, and S. Thrun, "Learning motion patterns of people for compliant motion," *Int. J. Robot. Res.*, vol. 24, no. 1, pp. 31–48, 2005.

[13] K. Madhava Krishna, R. Alami, and T. Simeon, "Safe proactive plans and their execution," *Robot. Auton. Syst.*, vol. 54, no. 3, pp. 244–255, Mar. 2006.

[14] A. Mandow, V. F. Mufloz, R. Fernandez, and A. Garcia-Cerezo, "Dynamic speed planning for safe navigation," in *Proc. Int. Conf. IROS*, 1997, pp. 231–237.

[15] K. Konolige, "A gradient method for realtime robot control," in *Proc. IEEE/RSJ Conf. Intell. Robots Syst.*, Takamatsu, Japan, 2000, pp. 639–646.

[16] S. Kim, W. Chung, C.-B. Moon, and J.-B. Song, "Safe navigation of a mobile robot using the visibility information," in *Proc. IEEE ICRA*, Rome, Italy, Apr. 2007, pp. 1304–1309.

[17] W. Chung, G. Kim, and M. Kim, "Development of the multi-functional indoor service robot PSR systems," *Auton. Robots*, vol. 22, no. 1, pp. 1–17, Mar. 2007.

[18] D. Lee and W. Chung, "Discrete status based localization for indoor service robots," *IEEE Trans. Ind. Electron.*, vol. 53, no. 5, pp. 1737–1746, Oct. 2006.

[19] G. Kim and W. Chung, "Tripodal schematic control architecture for integration of multi-functional indoor service robots," *IEEE Trans. Ind. Electron.*, vol. 53, no. 5, pp. 1723–1736, Oct. 2006.

[20] J. C. Latombe, *Robot Motion Planning*. Norwell, MA: Kluwer, 1991.

[21] O. Brock and O. Khatib, "High speed navigation using the global dynamic window approach," in *Proc. Int. Conf. Robot. Autom.*, 1999, pp. 341–346.

[22] R. C. Luo and K. L. Su, "Multilevel multisensor-based intelligent recharging system for mobile robot," *IEEE Trans. Ind. Electron.*, vol. 55, no. 1, pp. 270–279, Jan. 2008.

[23] F. J. Berenguer and F. M. Monasterio-Huelin, "Zappa, a quasi-passive biped walking robot with a tail: Modeling, behavior, and kinematic estimation using accelerometers," *IEEE Trans. Ind. Electron.*, vol. 55, no. 9, pp. 3281–3289, Sep. 2008.

[24] W. L. Xu, J.-S. Pap, and J. Bronlund, "Design of a biologically inspired parallel robot for foods chewing," *IEEE Trans. Ind. Electron.*, vol. 55, no. 2, pp. 832–841, Feb. 2008.


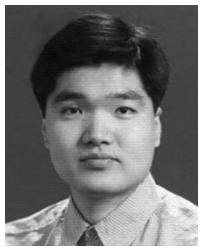

**Woojin Chung** (M'05) received the B.S. degree from the Department of Mechanical Design and Production Engineering, Seoul National University, Seoul, Korea, in 1993 and the M.S. and Ph.D. degrees from the Department of Mechano-Informatics, The University of Tokyo, Tokyo, Japan, in 1995 and 1998, respectively.

From 1998 to 2005, he was a Senior Research Scientist with the Korea Institute of Science and Technology. Since 2005, he has been with the Department of Mechanical Engineering, Korea University, Seoul. His research interests include the design and control of nonholonomic underactuated mechanical systems, trailer system design and control, and mobile robot navigation.

Dr. Chung received an Excellent Paper Award from the Robotics Society of Japan in 1996 and the King-sun Fu Memorial Best Transactions Paper Award from the IEEE Robotics and Automation Society in 2002.

**Seokgyu Kim** received the B.S. and M.S. degrees from the Department of Mechanical Engineering, Korea University, Seoul, Korea, in 2005 and 2007, respectively.

He is currently a Research Engineer with the Corporate Research and Development Division, Hyundai–Kia Motors, Gyeonggi-do, Korea. His research interests are intelligent navigation of robot/vehicle, human–machine interface, model-based design, and electric/electronic architecture in the automobile.

**Minki Choi** received the B.S. and M.S. degrees from the Department of Mechanical Engineering, Korea University, Seoul, Korea, in 2006 and 2008, respectively.

Since 2008, he has been a Research Scientist with the Intelligent System and Robotics Laboratory, Korea University. His research interests are mobile robot navigation algorithm, collision-free path generation, and sensor detection.

**Jaesik Choi** received the B.S. degree in computer engineering from Seoul National University, Seoul, Korea, in 2004. He is currently working toward the Ph.D. degree in the Department of Computer Science, University of Illinois, Urbana–Champaign.

From 2000 to 2003, he was a Lead Programmer with Somansa Company, Ltd., Seoul. From 2004 to 2005, he was a Research Programmer with Korea Institute of Science and Technology and Korea University. His research includes robot planning algorithms for manipulating objects, inference algorithms in hybrid graphical models, and image matching algorithms.

**Hoyeon Kim** received the B.S. degree from the Department of Mechanical Engineering, Korea University, Seoul, Korea, in 2008, where he is currently working toward the M.S. degree in robotics.

His research interests are mobile robot navigation, human robot interaction, and human following.

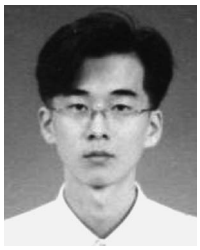

**Chang-bae Moon** received the B.S. and M.S. degrees from the School of Mechanical Engineering, Korea University, Seoul, Korea, in 2006 and 2008, respectively, where he is currently working toward the Ph.D. degree.

His research interests include mobile robot motion control, path planning, localization, and behavior selection.

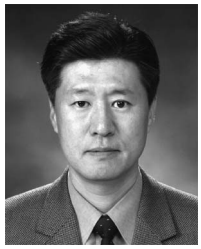

**Jae-Bok Song** (M'00) received the B.S. and M.S. degrees in mechanical engineering from Seoul National University, Seoul, Korea, in 1983 and 1985, respectively, and the Ph.D. degree in mechanical engineering from the Massachusetts Institute of Technology, Cambridge, in 1992.

In 1993, he joined the faculty of the Department of Mechanical Engineering, Korea University, Seoul, where he has been an Full Professor since 2002. Currently, he is the Director with the Intelligent Robotics Research Center, Korea University. His current research interests are safe manipulators, robot navigation, and design and control of the robotic systems including haptic devices and field robots.

Dr. Song is an Editor of *International Journal of Control, Automation, and Systems*.